A comparative study of spin coated and floating film transfer method coated poly (3-hexylthiophene)/poly (3-hexylthiophene)-nanofibers based field effect transistors

Shashi Tiwari, Wataru Takashima, S. Nagamatsu, S. K. Balasubramanian, and Rajiv Prakash

Citation: Journal of Applied Physics **116**, 094306 (2014); doi: 10.1063/1.4894458
View online: http://dx.doi.org/10.1063/1.4894458
View Table of Contents: http://scitation.aip.org/content/aip/journal/jap/116/9?ver=pdfcov
Published by the AIP Publishing

A comparative study of spin coated and floating film transfer method coated poly (3-hexylthiophene)/poly (3-hexylthiophene)-nanofibers based field effect transistors

Shashi Tiwari,[1] Wataru Takashima,[2] S. Nagamatsu,[3] S. K. Balasubramanian,[1] and Rajiv Prakash[4,a)]

[1]*Department of Electronics Engineering, Indian Institute of Technology (Banaras Hindu University), Varanasi 221005, India*
[2]*Research Center for Advanced Eco-fitting Technology, Graduate School of Life Science and Systems Engineering, Kyushu Institute of Technology, 2-4 Hibikino, Wakamatsu, Kitakyushu 808-0196, Japan*
[3]*Department of Computer Science and Systems Engineerings, Kyushu Institute of Technology, 680-4 Kawazu, Iizuka, Fukuoka 820-8502, Japan*
[4]*School of Materials Science and Technology, Indian Institute of Technology (Banaras Hindu University), Varanasi 221005, India*

(Received 4 August 2014; accepted 21 August 2014; published online 3 September 2014)

A comparative study on electrical performance, optical properties, and surface morphology of poly(3-hexylthiophene) (P3HT) and P3HT-nanofibers based "normally on" type p-channel field effect transistors (FETs), fabricated by two different coating techniques has been reported here. Nanofibers are prepared in the laboratory with the approach of self-assembly of P3HT molecules into nanofibers in an appropriate solvent. P3HT (0.3 wt. %) and P3HT-nanofibers (~0.25 wt. %) are used as semiconductor transport materials for deposition over FETs channel through spin coating as well as through our recently developed floating film transfer method (FTM). FETs fabricated using FTM show superior performance compared to spin coated devices; however, the mobility of FTM films based FETs is comparable to the mobility of spin coated one. The devices based on P3HT-nanofibers (using both the techniques) show much better performance in comparison to P3HT FETs. The best performance among all the fabricated organic field effect transistors are observed for FTM coated P3HT-nanofibers FETs. This improved performance of nanofiber-FETs is due to ordering of fibers and also due to the fact that fibers offer excellent charge transport facility because of point to point transmission. The optical properties and structural morphologies (P3HT and P3HT-nanofibers) are studied using UV-visible absorption spectrophotometer and atomic force microscopy , respectively. Coating techniques and effect of fiber formation for organic conductors give information for fabrication of organic devices with improved performance. © *2014 AIP Publishing LLC*. [http://dx.doi.org/10.1063/1.4894458]

INTRODUCTION

Field effect transistors (FETs) fabricated using conducting polymers as the active channel are gaining importance over the conventional thin film FETs mainly because of their high flexibility, light weight; easy in fabrication, and low cost.[1–4] Recent interest of the researchers is shown towards the modifications of organic semiconductors which can enhance the stability and performance of devices. Formation of nanocomposites, morphology control, and introduction of crystallinity/ordering are major focus due to achieving high surface to volume ratio and improved charge transfer characteristics. These may be easily achieved by using control polymer formation and deposition techniques. A variety of techniques such as catalytic synthesis, chemical vapour deposition, dilute polymerization, interfacial polymerization, and electrospinning can be used for the synthesis of polymer nanofibres with control size in and shape.[5–8]

Amongst the various organic conducting polymers, polyalkylthiophene and its derivatives are the most study polymers for fabrication of organic devices. Regioregular poly (3-hexylthiophene) (RR-P3HT),[9] one of the most popular polymer of polyalkylthiophene family, has been extensively studied for this purpose. It is extensively used for organic electronic devices because of its high charge carrier mobility, good processibility, efficient electronic and optical properties, and possibility for crystallization and nanofiber formation.[6]

Two methods are generally used for the formation of P3HT-nanofibers, viz., whisker method and mixed-solvent method.[7] In the whisker method, a polymer solution is prepared and then super cooled such that polymer chains get self-assembled and generate nanofibers. Further fibers are segregated from the super cooled suspension by filtration and centrifugation. Nanofiber morphology and dimensions are strongly dependent on solvent, polymer molecular weight and their regioregularity, solution concentration, and cooling rate.[6,7,10,11] Controlled morphology and dimensions of polymer nanofibers are a challenging issue. Mixed-solvent approach is another technique used for the preparation of

a)Author to whom correspondence should be addressed. Electronic mail: rajivprakash12@yahoo.com. Telephone: +91-9935033011.

P3HT-nanofibers.[12,13] In mixed-solvent technique, P3HT is dissolved in solvents like chlorobenzene (mild heating) and an appropriate amount of poor solvent (such as anisole) is added for promoting the precipitation of dissolved P3HT. Again the mixed solution is heated to get a well dissolved homogeneous solution state. The final solution is kept as the good solvent is the majority solvent and the poor solvent is the minority solvent. The cooling of the mixture induces some part of dissolving polymers into suspension state. Further some high molecular weight polymers start to solidify due to the effective $\pi-\pi$ stacking characteristics of P3HT. The existence of good solvent keeps the polymer into a stretched conformation and results the generated suspensions in a fiber-form. The aggregation of well-stretched polymer induces the crystallinity of thin-film casted from this solution. Therefore, such suspension effects on the electronic characteristics of organic devices like FET and solar cell. However, the electronic characteristics also depend further on the coating techniques used for fabrication of devices.

Single fiber P3HT-FET demonstrated high carrier mobility of 0.06 cm^2/V s as reported earlier[14,15] which is close to the mobility 0.25 cm^2/V s found in conventionally constructed P3HT-FET of similar design.[16] Recently, an excellent mobility of 2 cm^2/V s along with an on/off ratio of 10^5 has been reported for an electrospinning P3HT-nanofiber based FET in which polyelectrolyte was used as gate oxide instead of the conventional SiO_2.[17] Organic field effect transistors (OFETs) find numerous applications in modern electronics;[18–20] however, the progress in OFETs depends on many issues such as enhancement in device performance, decrement in fabrication cost, and expansion in the area of applications.

Simple spin coating technique is one of the most common methods used for the deposition of film to fabricate device at low cost.[21–23] Thickness of the spin coated film depends on various factors like the solvent used, solution concentration, and its viscosity. It also depends on the spin coating parameters such as speed, acceleration, and coating time.

Floating film transfer method (FTM) is another unique casting-process recently developed by our group with the target to get highly uniform thin-film by an easy approach.[24,25] In this technique, a drop of polymer solution was put on the top of a hydrophilic liquid viscous surface; the drop of the hydrophobic polymer solution spread as a thin-film on this viscous surface substrate. This floating film can be transferred on various substrates by placing the face of these substrates on the film and then taking it out like Langmuir-Schaefer method.[26] Thin-film of polymer deposited by FTM has very good uniformity with a large level of self-orientation of the polymeric molecules without any external force and also has the benefit of less residual stress due to the use of liquid viscous surface as primary substrates compared to solid substrates, whereas films deposited on solid substrates were reported to have increasing stress during solidification. Film parameters (thickness and morphology) deposited by FTM can be controlled by controlling the viscosity and temperature of the liquid. Transport characteristics were also observed in the thin-films prepared by FTM.[24,25] In spin coating technique, approximately 80% polymer solution get waste during the coating. It is reported earlier that the X-ray diffraction and atomic force microscope measurements showed much better ordering for the FTM films in comparison to spin-coated films. It is also found that the transport characteristics, on/off ratio and threshold voltage improved for organic films formed by FTM methods in comparison to any other conventional techniques like drop casting or spin coating, etc.[24,25]

In view of above, we report a comparative study on the electrical performance of FETs fabricated using P3HT and P3HT-nanofiber as active channel deposited by spin coating and FTM. The structural morphology and optical properties of P3HT and P3HT-nanofibers were also compared for device performance.

EXPERIMENTAL DETAILS

RR-P3HT was synthesized in the laboratory and method adopted in its synthesis has been earlier reported.[27,28] A consistent solution of RR-P3HT in dehydrated toluene with concentration 1 wt. % was prepared by heat treatment. After cooling at room temperature, the solution was stored in a firmly sealed glass vessel for 45 days at a constant temperature (25 °C). Gradually, P3HT molecules come together by the driven force of $\pi-\pi$ interchain stacking and fuse in the form of suspended nanofibers. Physical changes in the viscosity and color of this solution was observed day by day, and after 45 days, the solution appeared dark purple-brownish color with increased viscosity; however, initially (before 45 days) it was dark-orange color with less viscosity. These suspended nanofibers were segregated by centrifuging the suspension at 6000 rpm for 30 min. The accumulated solid parts were taken out and re-dispersed in dehydrated chloroform before drying. The concentration of this suspension was calculated to be 0.25 wt. % by using the UV-visible absorption characteristics of the P3HT-solutions of known concentrations as shown in Figs. 2(a) and 2(b), which is also discussed in result parts. This fiber suspension was used for the fabrication of OFETs.

Prior to spin coating or FTM deposition, this suspension was re-dispersed thoroughly with a cyclo-mixer. p-doped silicon species of dimension 1 cm × 1 cm along with thermally grown SiO_2 ($C_{ox} = 10$ nF/cm^2) layer (300 nm) were used as base substrate for OFETs. Cyclo-mixed fiber suspension was spin coated on the substrate (p^+-Si/SiO_2) with 1000 rpm for 10 s followed by 3000 rpm for 50 s. The film thickness was varied from 65 to 70 nm measured with DEKTAK 6 M Profiler. Further, few substrates (p^+-Si/SiO_2) were coated with FTM, in which a drop (nearly 30 μl as optimized for film thickness) of cyclo-mixed nanofiber suspension was put on the top of a viscous hydrophilic liquid surface on a mixture of ethylene glycol and glycerol (ratio 1:2). The drop quickly spread as thin-film over liquid viscous surface. The formed floating film was transferred on silicon substrates (p^+-Si/SiO_2) by placing the face of these substrates on the film and then carefully lifting them. The thickness of FTM coated thin-film was measured in the range from 35 to 40 nm (optimized film thickness), which was depending on the

polymer concentration, temperature, and viscosity of the hydrophilic liquid surface and ratio of the mixture of ethylene glycol and glycerol. Thickness was controlled by controlling these parameters and optimum was used to get high charge mobility.

Further, by using Ni-shadow mask, two gold electrodes (source-drain) of thickness 40 nm were subsequently deposited at the top of the coated thin-film with thermal vapour deposition technique at vacuum pressure of 3×10^{-6} Torr. The channel lengths and width of FETs were maintained 20 μm and 2 mm, respectively. In a similar way, few FETs based on P3HT/$CHCl_3$ (0.3 wt. %) were also prepared under identical conditions as mentioned above to compare their performance with P3HT-nanofiber FETs. Electrical characteristics of fabricated OFETs were measured through a Keithley 2612 two channel electrometer at vacuum pressure of 4×10^{-6} Torr. The optical properties and microstructure of P3HT and P3HT-nanofiber thin-films were studied by measuring UV-visible absorption spectra (JASCO V-750 spectrophotometer) and atomic force microscopy (AFM) (JEOL SPM5200), respectively.

RESULTS AND DISCUSSION

Formation of nanofiber was confirmed by analysis of UV-visible absorption spectra and AFM microstructures. Observed morphology and absorption peak heights for both P3HT and P3HT-nanofibers were drastically different as also discussed ealier.[29] The UV-visible absorption spectra for solution, nanofiber suspension is compared in Fig. 1 (inset). A single absorption peak for P3HT solution in chloroform was observed at wavelength of 450 nm; however, five distinct peaks intensities at wavelengths of 460 nm, 480 nm, 520 nm, 560 nm, and 610 nm were observed for P3HT-nanofiber suspension as discussed ealier.[29] The relative high and sharp peaks of long wavelength at 560 nm and 610 nm represent a well-stretched conjugation length due to better π–π stacking in P3HT chain to form nanofibers. This means that the prepared nanofiber suspension possesses good ordering of the polymer chains, and poor solubility even in chloroform at room temperature. It was further confirmed as on heating the solution fibers completely dissolved and UV-vis absorption showed similar spectrum as for P3HT solution (cf. Fig. 1). The concentration of the nanofiber suspension was calculated in the same way as reported in our previous paper.[29] Two different concentrations of P3HT solutions gave different peak-heights at the wavelength of 450 nm as shown in Fig. 1 and an unknown quantity of nanofiber suspension (used in device fabrication) diluted 150 times with chloroform (fully dissolved nanofibers homogeneous solution achieved after heating) also gave same peak with different height (ignoring slight shift in peak position). Unknown was calculated as 0.25 wt. % using two point calibration plot as shown in Fig. 2.

The UV-absorption peak for this nanofiber dissolved solution showed a little red-shifted as compared to that of P3HT-solutions. This shift is due to the fact that, during fiber formation only higher molecular weight P3HT molecules get self-assembled and join together as nanofibers, whereas low molecular weight P3HT molecules failed to form fibers. These nanofibers from low molecular weight dissolved P3HT solution were segregated by centrifuging the suspension. Therefore, re-dispersed nanofibers in chloroform exhibit little longer wavelength as appears in Fig. 1, which verifies that the suspended solid parts were nanofibers.

The growth of nanofibers was further confirmed by AFM characterization. The AFM of P3HT and P3HT-nanofiber thin-film deposited by spin coating as well as by FTM were measured by scanning the film area of 5 μm × 5 μm, shown in Figs. 3(a)–3(d). In comparison, it was found that the morphology of spin coated and FTM coated P3HT thin-film appeared very different.

Spin coated P3HT molecules were spherical in shape with diameter range of 15 to 20 nm [Fig. 3(c)], whereas FTM coated P3HT thin-film did not show any particular features

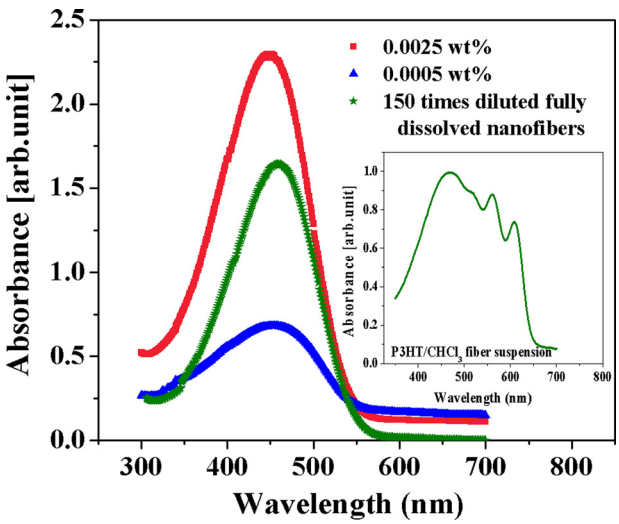

FIG. 1. UV-visible absorption spectra for various P3HT solutions of distinct concentrations; Green curve exhibits the UV-vis. absorption spectra of fully dissolved P3HT-nanofiber solution after heat treatment, Inset: UV-visible absorption spectra for P3HT solution, spin-coat P3HT film, and P3HT-nanofiber suspension in chloroform.

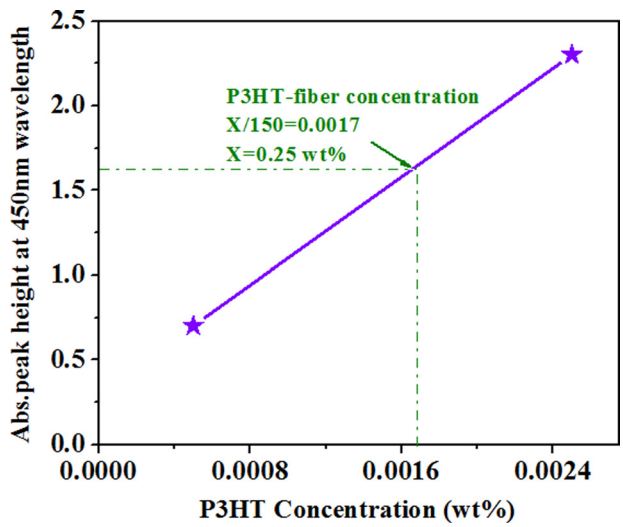

FIG. 2. Absorption peak height at 450 nm versus P3HT concentration (wt. %): green dotted line is drawn for dissolved P3HT-nanofiber solution through which concentration of nanofiber/chloroform suspension was estimated about 0.25 wt. %.

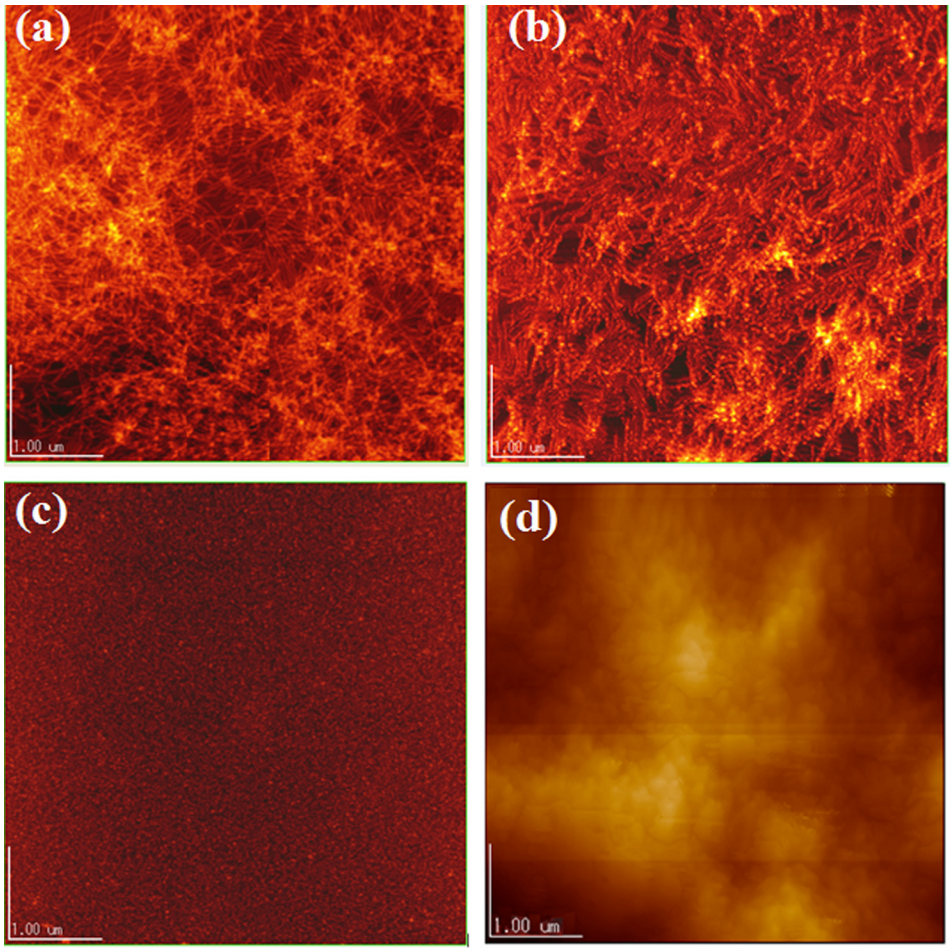

FIG. 3. AFM images for thin-film of (a) spin coated P3HT-nanofibers, (b) FTM coated P3HT-nanofibers, (c) spin coated P3HT solution, and (d) FTM coated P3HT solution.

[Fig. 3(d)]. Similarly, in spin coated P3HT-nanofibers thin-film, nanofibers were clearly visible and their dimensions such as length and diameter varied in the range of 500 to 700 nm and 10 to 12 nm, respectively, as shown in Fig. 3(a). This film (spin coated P3HT-nanofibers) showed good uniformity and also depicted some degree of fiber orientation due to the centrifugal force acting along the substrate during coating.

On the other hand, the FTM coated P3HT nanofiber thin-film showed excellent uniformity than spin coated nanofiber film. One more interesting observation in FTM coated P3HT nanofiber thin-film was noticed that a large degree of self-alignment in the polymer nanofibers was occurred which can clearly seen in Fig. 3(b). The range for length and diameter of the FTM coated P3HT-nanofibers was observed to be 400 to 700 nm and 10 to 15 nm, respectively.

The typical current-voltage characteristics of spin coated and FTM coated channel of P3HT and P3HT-nanofiber based FETs are shown in Figs. 4(a)–4(d) and Figs. 5(a)–5(d). The non-linear drain-source current (I_{DS}) versus drain-source voltage (V_{DS}) characteristics (output characteristics) at fixed gate-source voltage (V_{GS}) have two regions, linear and saturation regions. In the linear region, transition in I_{DS} depends on V_{DS} described though a parabola and in the saturation region, I_{DS} was independent of V_{DS}. The output characteristics of nanofiber-based FETs are shown in Fig. 4, and those of solution-based FET are shown in Fig. 5, respectively. Other information regarding the device performance such as ON/OFF ratio, threshold voltage (V_{TH}) could be extracted from the transfer characteristics drawn for I_{DS} versus V_{GS} at fixed $V_{DS} = -80$ V which are depicted in Figs. 4(b) and 4(d) for spin coated and FTM coated nanofiber based FETs, respectively, and for P3HT FETs, it is depicted in Figs. 5(b) and 5(d), respectively. ON/OFF current ratio characterizes the switching performance estimated by the maximum I_{DS} in accumulation mode divided by the minimum I_{DS} in depletion mode at the same voltage regime. This ratio is generally influenced by the conducting capability.[30] The threshold voltage (V_{TH}) for a device is the apparent voltage required for starting the ON-state from their OFF-state. In case of OFET, V_{TH} can be calculated by the linear fit of $I_{DS}{}^{1/2}$ versus V_{DS} curve which intersects the x-axis at a point where I_{DS} is zero.[31–33] The mobility is another key parameter of the OFET which is defined as the charge carrier velocity per unit applied electric field.[34] The field-effect carrier mobility in the saturation region (μ_{sat}) can be found by using the expression (1)[35,36] and the conductance (S) can be determined by expression (2):[37]

$$\sqrt{I_{DS}} = \sqrt{\frac{W\mu_{sat}C'_{ox}}{2L}}(V_{GS} - V_{TH}) \tag{1}$$

$$S = \frac{W\mu_{sat}C_{ox}}{L}(V_{GS} - V_{TH}), \tag{2}$$

where W and L are the channel length and width, respectively, for the FET, and Cox is the gate oxide capacitance per unit

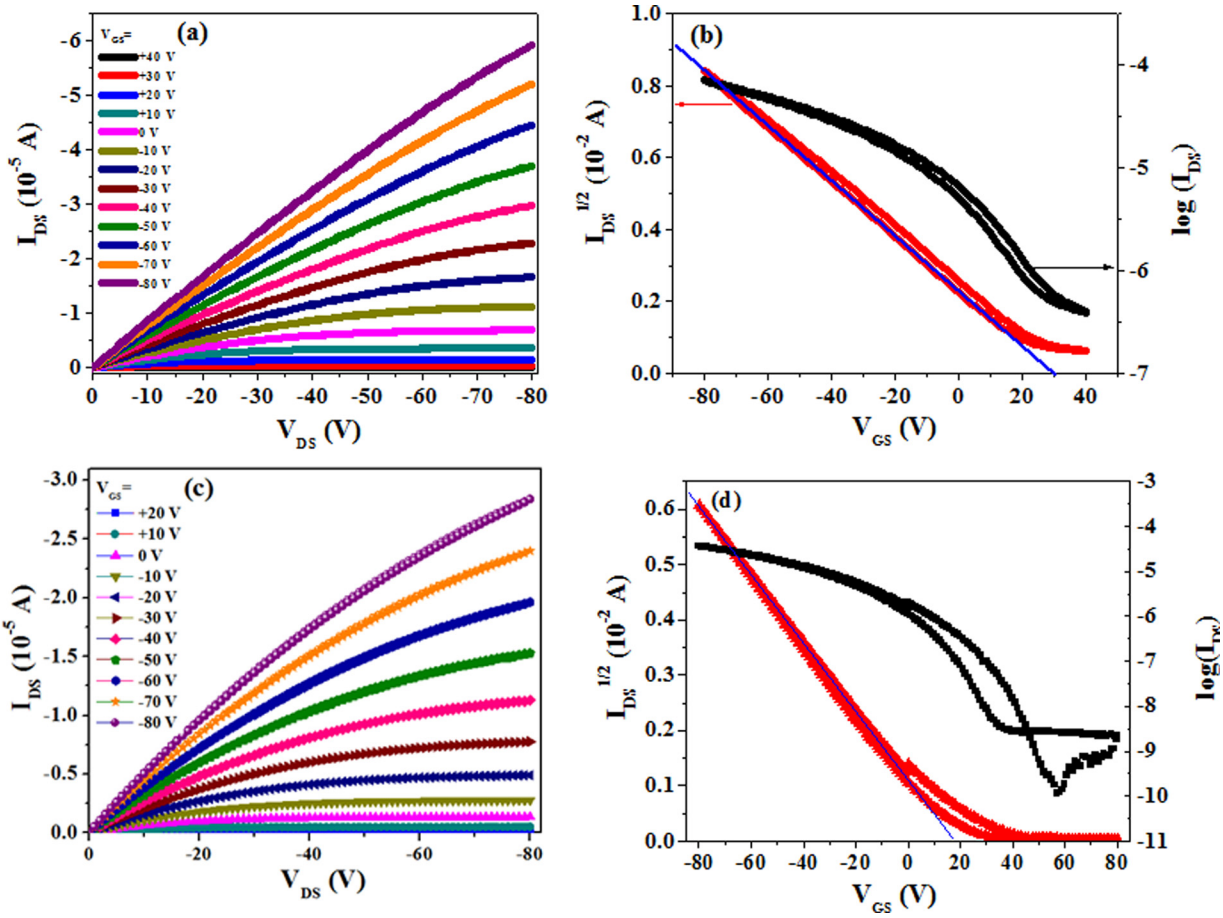

FIG. 4. Current-Voltage (I-V) characteristics of spin coated and FTM coated P3HT-nanofiber FETs (a) spin coated output characteristics (I_{DS} vs V_{DS}), (b) spin coated transfer characteristics, (I_{DS} vs V_{GS}) and [log(I_{DS}) vs V_{GS}], (c) FTM coated output characteristics, (d) FTM coated transfer characteristics, (I_{DS} vs V_{GS}) and [log(I_{DS}) vs V_{GS}].

area. The possible key performance parameters such as μ_{sat}, ON/OFF ratio, V_{TH} and S for all fabricated OFETs were calculated by using the above discussion and formulae, and values are listed in Table I. By analyzing the calculated parameters listed in Table I, it was concluded that the performances of P3HT-nanofiber based FETs were much superior than those of the solution coated P3HT FETs, though, concentration of fiber suspension (used at FET channel) was less (0.25 wt. %) compared to P3HT solution concentration (0.3 wt. %). Therefore, the use of nanofibers as active channel for OFETs was advantageous in two aspects, namely, (1) high device performance and (2) less material consumption. The field-effect mobility of spin coated P3HT-nanofiber FET was found to be 9.15×10^{-3} cm^2/V s. This value was quite comparable to the mobility value of 6.26×10^{-3} cm^2/V s calculated for FTM coated P3HT-nanofiber FET. The surface morphology of spin coated nanofibers at FET channel shows some degree of fiber orientation due to centrifugal force acting over the substrate during spin coating. Such orientations cause some extent of alignment in the nanofibers; due to this fact, it was assumed that the aligned nanofibers might provide direct swift lanes for the hole carriers for point to point transportation which would enhance the carrier transport property of the spin coated fiber thin-film.[39] Thickness and uniformity of this film was also sufficient enough to transport large number of holes from the FET channel.

On the other hand, excellent uniformity was observed in the floating film which was deeply depend on the driving force by which polymer solution spread uniformly over the hydrophilic viscous substrate and also depends on the resistive force offered by the solidification of the thin-film. Another interesting thing in FTM was observed that the fabricated thin-film of P3HT-nanofiber shows a great extent of self-alignment of the nanofibers in the film without any external force. These alignments in the P3HT-nanofibers depend on the nanofiber suspension propagation speed and the rate of film solidification. Such uniformity and alignments in the fiber thin-film boost the carrier transport property of the film. Therefore, excellent transport property in FTM coated P3HT-nanofiber FET was observed which strongly depends on the thin-film morphology, microstructure, and control of polymer orientation in the active channel film.[38] Therefore, compared to spin coated P3HT-nanofiber thin-film, the surface morphology of the FTM coated P3HT-nanofiber thin-film shows excellent uniformity and fiber alignment which drastically improve the FTM coated P3HT-nanofiber FET performance. The thickness of the FTM coated channel film was measured and found to be around 35–40 nm.

The ON/OFF current ratio of the FTM coated FETs was much better compared to the spin coated one, and values are listed in Table I. The best ON/OFF ratio of approximately

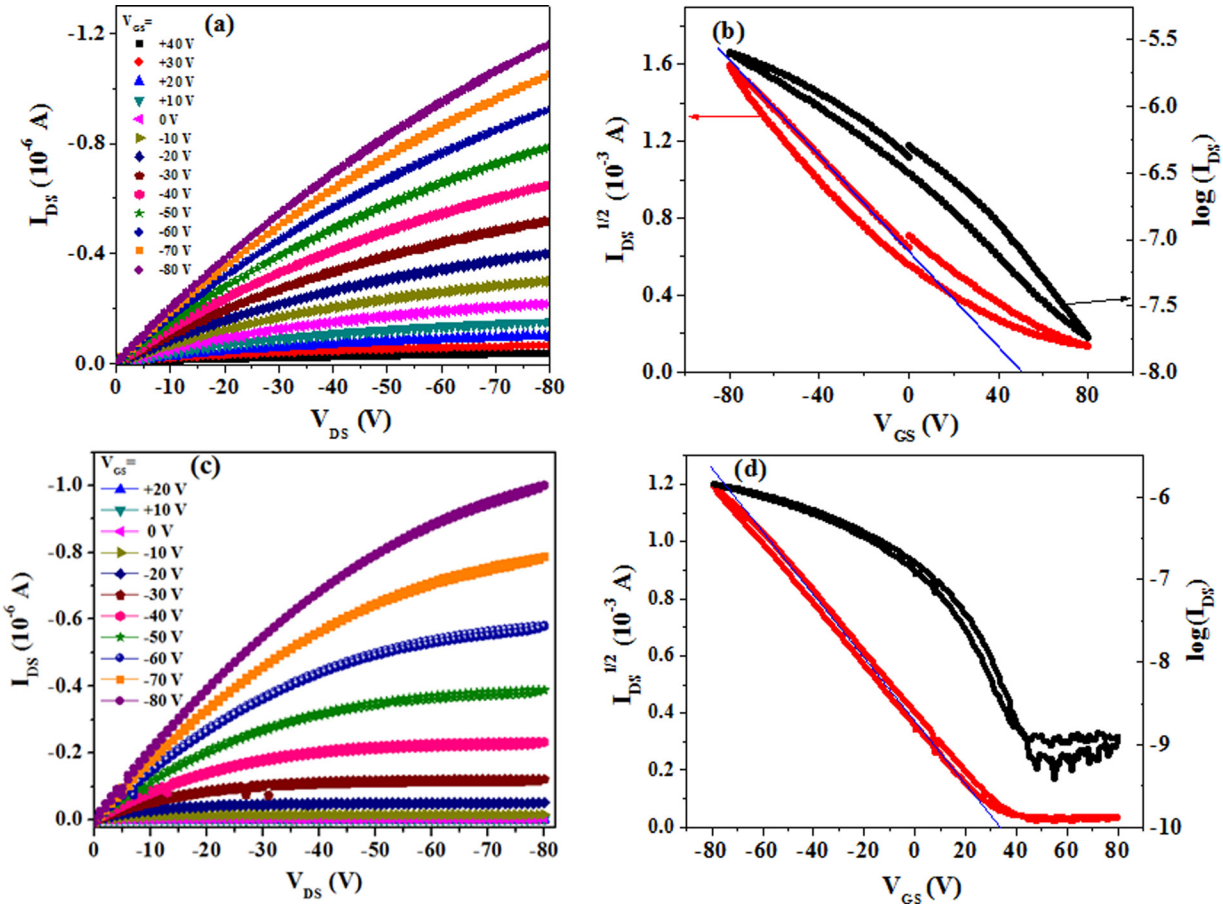

FIG. 5. Current-Voltage (I-V) characteristics of spin coated and FTM coated P3HT FET (a) spin coated output characteristics (I_{DS} vs V_{DS}), (b) spin coated transfer characteristics, (I_{DS} vs V_{GS}) and [log(I_{DS}) vs V_{GS}], (c) FTM coated output characteristics, and (d) FTM coated transfer characteristics, (I_{DS} vs V_{GS}) and [log(I_{DS}) vs V_{GS}].

10^5 was measured for FTM coated P3HT-nanofiber FET which was approximately two orders higher compared to the ON/OFF current ratio of the spin coated nanofiber FET. The "ON" current in both (FTM and spin coated) type OFETs was comparable; however, "OFF" current in FTM coated FETs was very small compared to "OFF" current in spin coated FETs. This may be because that many parts of PHT domain well contact to gate insulator for FTM film with thanks to their well alignment, which provides whole the channel are sensitive to the gate voltage to control the carrier number by the field-effect. Therefore, ON/OFF current ratio for FTM coated OFETs was measured higher compared to the spin coated OFETs.

TABLE I. Key parameters of P3HT and P3HT-nanofibers based FETs fabricated by two techniques i.e. spin coating and FTM.

Channel	V_{TH} (V)	μ_{sat} (cm^2/Vs)	ON/OFF ratio	Conductance (S)	H_I %
Nanofiber-based FET with spin-coat	30	9.15×10^{-3}	$10^{2.3}$	1.1×10^{-6}	18
Nanofiber-based FET with FTM	17	6.26×10^{-3}	10^{5}	0.56×10^{-6}	5
Solution-based FET with spin-coat	50	2.11×10^{-4}	10^{2}	2.74×10^{-8}	20
Solution-based FET with FTM	32	1.07×10^{-4}	$10^{3.2}$	1.61×10^{-8}	7

Cyclic transfer characteristics of each FETs depicted little hysteresis loop. Hysteresis is frequently noticed in OFETs during sweeping of V_{GS}. The reason of hysteresis is mainly due to the fact that the charge trapping density occurred at the organic semiconductor/insulator interface and sometimes the presence of impurities (like water molecules) in the solvent or in the organic semiconductor also induces hysteresis.[29,31,40,41] Origin of hysteresis deteriorates the switching function for FET, so, it should be minimized by avoiding the source of their origin. Hysteresis Intensity % (H_I%) in each OFET can be evaluated by using mathematical equation:[29]

$$H_I\% = \left(\frac{I_{DS,end} - I_{DS,start}}{I_{DS,start}}\right) \times 100, \quad (3)$$

where $I_{DS,start}$ and $I_{DS,end}$ are the initial and final drain-source current observed at $V_{GS} = 0$ V, during cyclic transfer measurement. Table I shows the coating method changes H_I intensity. Even to coat the film from the different structured solutions (namely, well-dissolved solution and nanofiber dispersion), FTM coating channel provides small H_I as compared to those from spin-coat channel. It should be noted that both of these solutions are prepared from the same P3HT and solvent. In addition, FTM is the procedure to cast P3HT on hydrophilic liquid. These facts indicate that the origin to cause the hysteresis appeared in these transfer characteristics is not in some impurities in solution and suspension

but in the casting procedure to provide the P3HT film. A possible explanation is that the FTM provides to cast P3HT nanofibers and macromolecules into well-aligned form for eliminating nano-space or minimizing amorphous regime. This also contributes to realize the strong off-state due to the effective eject of carriers at relative small V_{TH} even in these normally on state channels.

CONCLUSION

Spin coated and FTM coated channels of P3HT-nanofibers and P3HT based FETs were prepared to compare their performance. The electrical performance parameters of FETs were strongly dependent on the channel material and thin-film surface morphology. The carrier mobility of both coating techniques based OFETs were comparable; however; drastic changes in on/off ratio, threshold voltage, hysteresis intensity were found for two different coating methods. The best on/off ratio of 10^5 was estimated for the FTM coated P3HT-nanofibers FET. This value was approximately two to three orders higher than the on/off ratio of all other FETs fabricated by FTM and spin coating techniques reported earlier. Threshold voltage and hysteresis intensity of the same device (FTM coated P3HT-nanofibers FET) was also much better compare to other OFETs. It is concluded that P3HT-nanofiber FET shows superior electrical performance than the other fabricated FETs due to the fact that the nanofibers probably provide "swift lanes" for end-to-end charge carrier transportation.

[1]Y. Xu, T. Minari, K. Tsukagoshi, J. A. Chroboczek, and G. Ghibaudo, J. Appl. Phys. **107**, 114507 (2010).
[2]S. Tiwari, A. K. Singh, L. Joshi, P. Chakrabarti, W. Takashima, K. Kaneto, and R. Prakash, Sens. Actuators B **171–172**, 962 (2012).
[3]Y. Li, C. Liu, Y. Wang, Y. Yang, X. Wang, Y. Shi, and K. Tsukagoshi, AIP Adv. **3**, 052123 (2013).
[4]W. O. Yang, M. Weis, D. Taguchi, X. Chen, T. Manaka, and M. Iwamoto, J. Appl. Phys. **107**, 124506 (2010).
[5]L. M. Colangelo and A. J. Baeumner, Lab Chip **12**, 2612 (2012).
[6]W. D. Oosterbaan, V. Vrindts, S. Berson, S. Guillerez, O. Douheret, B. Ruttens, and J. D. Peter, J. Mater. Chem. **19**, 5424 (2009).
[7]S. Sun, T. Salim, L. H. Wong, Y. L. Foo, F. Boeya, and Y. M. Lam, J. Mater. Chem. **21**, 377 (2011).
[8]S. B. Jo, W. H. Lee, L. Qiu, and K. Cho, J. Mater. Chem. **22**, 4244 (2012).
[9]P. Cosseddu, S. Milita, and A. Bonfiglio, IEEE Electron Device Lett. **33**, 113 (2012).
[10]J. Liu, M. Arif, J. Zou, S. I. Khondaker, and L. Zhai, Macromolecules **42**, 9390 (2009).
[11]K. Zhao, L. Xue, J. Liu, X. Gao, S. Wu, Y. Han, and Y. Geng, Langmuir **26**, 471 (2010).
[12]L. Li, G. Lu, and X. Yang, J. Mater. Chem. **18**, 1984 (2008).
[13]N. Kiriy, E. Jahne, H. J. Adler, M. Schneider, A. Kiriy, G. Gorodyska, S. Minko, D. Jehnichen, P. Simon, A. A. Fokin, and M. Stamm, Nano Lett. **3**, 707 (2003).
[14]J. A. Merlo and C. D. Frisbie, J. Polym. Sci. **41**, 2674 (2003).
[15]J. A. Merlo and C. D. Frisbie, J. Phys. Chem. B **108**, 19169 (2004).
[16]S. Cho, K. Lee, J. Yuen, G. Wang, D. Moses, A. J. Heeger, M. Surin, and R. Lazzaroni, J. Appl. Phys. **100**, 114503 (2006).
[17]S. W. Lee, H. J. Lee, J. H. Choi, W. G. Koh, J. M. Myoung, J. H. Hur, J. J. Park, J. H. Cho, and U. Jeong, Nano Lett. **10**, 347 (2010).
[18]H. N. Raval, S. P. Tiwari, R. R. Navan, S. G. Mhaisalkar, and V. Ramgopal Rao, IEEE Electron Device Lett. **30**, 484 (2009).
[19]H. Sirringhaus, N. Tessler, and R. H. Friend, Science **280**, 1741 (1998).
[20]B. Crone, A. Dodabalapur, A. Gelperin, L. Torsi, H. E. Katz, A. J. Lovinger, and Z. Bao, Appl. Phys. Lett. **78**, 2229 (2001).
[21]Y. Li, C. Liu, A. Kumatani, P. Darmawan, T. Minari, and K. Tsukagoshi, Org. Electron. **13**, 264 (2012).
[22]C. Liu, T. Minari, X. B. Lu, A. Kumatani, K. Takimiya, and K. Tsukagoshi, Adv. Mater. **23**, 523 (2011).
[23]Y. Li, C. Liu, Y. Xu, T. Minari, P. Darmawan, and K. Tsukagoshi, Org. Electron. **13**, 815 (2012).
[24]T. Morita, V. Singh, S. Nagamatsu, S. Oku, W. Takashima, and K. Kaneto, Appl. Phys. Exp. **2**, 111502 (2009).
[25]R. K. Pandey, W. Takashima, S. Nagamatsu, A. Dauendorffer, K. Kaneto, and R. Prakash, J. Appl. Phys. **114**, 054309 (2013).
[26]R. K. Pandey, C. Upadhyay, and R. Prakash, RSC Adv. **3**, 15712 (2013).
[27]M. Jeffries, G. Sauve, and R. D. McCullough, Macromolecules **38**, 10346 (2005).
[28]M. Trznadel, A. Pron, M. Zagorska, R. Chrzaszcz, and J. Pielichowski, Macromolecules **31**, 5051 (1998).
[29]S. Tiwari, W. Takashima, S. K. Balasubramanian, S. Miyajima, S. Nagamatsu, S. S. Pandey, and R. Prakash, Jpn. J. Appl. Phys., Part 1 **53**, 021601 (2014).
[30]J. C. Hsu, W. Y. Lee, H. C. Wu, K. Sugiyama, A. Hirao, and W. C. Chen, J. Mater. Chem. **22**, 5820 (2012).
[31]M. M. Torrent and C. Rovira, Chem. Rev. **111**, 4833 (2011).
[32]Y. W. Lin, C. J. Lin, Y. H. Chou, C. L. Liu, H. C. Chang, and W. C. Chen, J. Mater. Chem. C **1**, 5336 (2013).
[33]H. Sinno, S. Fabiano, X. Crispin, M. Berggren, and I. Engquist, Appl. Phys. Lett. **102**, 113306 (2013).
[34]H. E. Katz and J. Huang, Annu. Rev. Mater. Res. **39**, 71 (2009).
[35]J. H. Huang, C. Y. Yang, C. Y. Hsu, C. L. Chen, L. Y. Lin, R. R. Wang, K. C. Ho, and C. W. Chu, ACS Appl. Mater Interface **1**, 2821 (2009).
[36]S. Tiwari, A. K. Singh, and R. Prakash, J. Nanosci. Nanotechnol. **14**, 2823 (2014).
[37]R. S. Dudhea, J. Sinha, A. Kumar, and V. R. Rao, Sens. Actuators B **148**, 158 (2010).
[38]K. Sakamoto, T. Yasuda, K. Miki, M. Chikamatsu, and R. Azumi, J. Appl. Phys. **109**, 013702 (2011).
[39]U. Bielecka, P. Lutsyk, K. Janus, J. Sworakowski, and W. Bartkowiak, Org. Electron. **12**, 1768 (2011).
[40]W. Huang, W. Shi, S. Han, and J. Yu, AIP Adv. **3**, 052122 (2013).
[41]K. Tetzner, W. Duffy, and K. Bock, Appl. Phys. Lett. **103**, 093304 (2013).